2.3 A mathematical formulation of the Yarkovsky/YORP effect

The goal of this section is to present, at first, a very simple analytical solution of the 1-dimensional heat diffusion equation, which allows us to quantitatively estimate the Yarkovsky acceleration. This solution, thougth being simple and clear, holds basic properties of the Yarkovsky effect, such as its dependence on material, the rotational or orbital frequency; we also discuss the dependence on size and obliquity. We follow the analysis by Bertotti, Farinella & Vokrouhlický (2003) here. There is a description of the spherically symmetric solution by Vokrouhlický (1998), Vokrouhlický & Farinella (1999) and Vokrouhlický (1999) in the second part, supplemented by notes on its implementation in the `swift_rmvsy` *numerical integrator package, which we usually use for numerical simulations involving the Yarkovsky effect.*

How do we calculate the Yarkovsky/YORP effect? In order to estimate the recoil force and momentum acting on an asteroid, which emits thermal radiation, we need to know, at first, the temperature distribution on its surface. A rough estimate of the mean *equilibrium* temperature $T_{\rm eq}$ can be obtained easily, if we assume the asteroid is in the thermal equilibrium:

$$\pi R^2(1-A)\frac{L_\odot}{4\pi r^2} = 4\pi R^2 \epsilon\sigma T_{\rm eq}^4\,, \tag{1}$$

where A denotes the Bond albedo, $L_\odot \doteq 3.83\times 10^{26}\,\mathrm{W}$ the solar radiation power, r the distance from the Sun, ϵ the infrared emissivity, σ the Stefan-Boltzmann constant (the radius R is not important). If we drop the number 4 from Eq. (1), we get the 'noon' subsolar temperature $T_\star = \sqrt{2}\,T_{\rm eq}$. For (2953) Vysheslavia (with $r \simeq a = 2.83\,\mathrm{AU}$ and $A \simeq 0.2$; discussed in Sec. 4) we have $T_{\rm eq} \doteq 160\,\mathrm{K}$ and $T_\star \doteq 220\,\mathrm{K}$.

Of course, a more realistic situation is more complicated — in order to find the temperature $T(\mathbf{r},t)$, as a function of the position $\mathbf{r}$ and time t, we have to solve a heat diffusion equation in the volume of the body:

$$\nabla\cdot(K\nabla T) = \rho C\frac{\partial T}{\partial t}\,, \tag{2}$$

with a boundary condition on the surface:

$$\left(K\frac{\partial T}{\partial r}\right)_{\rm surface} + \epsilon\sigma T^4 = (1-A)\,\boldsymbol{\mathcal{E}}(t)\cdot\mathbf{n}_\perp(\mathbf{r})\,, \tag{3}$$

where K denotes the thermal conductivity, ρ the density, C the specific thermal capacity and $\mathcal{E}(t)$ the time dependent radiation flux (with respect to the local normal; $\mathcal{E}(t)$ differs from 0 only when the scalar product $\boldsymbol{\mathcal{E}}\cdot\mathbf{n}$ is positive).

2.3.1 A 1-dimensional toy model.

To keep things as clear as possible, let us consider a 1-dimensional example: an half-space $x \geq 0$ of a homogeneous material irradiated by a periodic flux $\mathcal{E}(t) = \mathcal{E}_0 + \mathcal{E}_1\,\mathrm{e}^{\mathrm{i}2\pi f t}$, i.e., 'something like' alternating day and night. (Only the real part $\mathrm{Re}\{\mathcal{E}\} = \mathcal{E}_0 + \mathcal{E}_1\cos 2\pi f t$ is relevant.) We can imagine, this is a single thin 'column' of a big asteroid, with the surface element irradiated by the Sun, which changes its position on the sky. (The frequency f can characterise either the diurnal or the seasonal motion.) The heat diffusion equation (2) and the boundary condition (3) then read:

$$\chi\frac{\partial^2 T}{\partial x^2} = \frac{\partial T}{\partial t}\,, \tag{4}$$

$$-K\frac{\partial T}{\partial x} + \epsilon\sigma T^4 = (1-A)\mathcal{E}(t)\,, \tag{5}$$

where $\chi = \frac{K}{\rho C}$ is the thermal diffusivity of the material. In general, we want to find the temperature $T(x,t)$ as a function of the depth and time.

Because $\mathcal{E}(t)$ is a harmonic function, we 'guess' the response of T, in *steady state*, will be analogous. Thus, we try to find a particular solution of the form $T(x,t) = T_0 + T_1(x)\,\mathrm{e}^{\mathrm{i}2\pi f t}$. ($T_1(x)$ might be a complex function, which would mean a phase shift of the temperature with respect to the incident radiation.) The Eq. (4) then reduces to an ordinary differential equation for $T_1(x)$:

$$\frac{\mathrm{d}^2 T_1}{\mathrm{d}x^2}(x) = \frac{\mathrm{i}2\pi f}{\chi}T_1(x)\,, \tag{6}$$

Table 5: Typical assumed values of the material thermal parameters we use for modelling of the Yarkovsky/YORP effect. ϱ_{bulk} denotes the bulk density, ϱ_{surf} the surface density, K the thermal conductivity, C the specific thermal capacity, and A the albedo.

material	ϱ_{bulk} $\mathrm{kg\cdot m^{-3}}$	ϱ_{surf} $\mathrm{kg\cdot m^{-3}}$	K $\mathrm{W\cdot m^{-1}\cdot K^{-1}}$	C $\mathrm{J\cdot kg^{-1}\cdot K^{-1}}$	A
bare basalt	3500		0.5–2.5	680	0.1–0.16
regolith covered	3500	1500	0.001–0.01	680	
metal	8000		~ 40	500	0.09–0.11
C-type	1000		0.1–1	1500	0.03–0.08

which non-divergent solution we find easily:

$$T_1(x) = T_1(0)\,\mathrm{e}^{-\sqrt{\mathrm{i}2\pi f/\chi}\,x} = T_1(0)\,\mathrm{e}^{-(1+\mathrm{i})\sqrt{\pi f/\chi}\,x}\,. \tag{7}$$

We see the *changes* of the temperature decrease with depth as $\mathrm{e}^{-\frac{x}{\delta}}$ and the penetration depth of the thermal wave is of the order $\delta = \sqrt{\chi/(\pi f)}$. (And, moreover, there is some phase shift too.)

We still do not know the surface temperature $T(0,t)$. Here, we exploit the boundary condition (Eq. 5), where we substitute the already known derivative $\frac{\partial T}{\partial x}(x,t) = -(1+\mathrm{i})\sqrt{\pi f/\chi}\,T_1(x)\,\mathrm{e}^{\mathrm{i}2\pi f t}$, so

$$K(1+\mathrm{i})\sqrt{\pi f/\chi}\,T_1(0)\,\mathrm{e}^{\mathrm{i}2\pi f t} + \epsilon\sigma(T_0 + T_1(0)\,\mathrm{e}^{\mathrm{i}2\pi f t})^4 = (1-A)(\mathcal{E}_0 + \mathcal{E}_1\,\mathrm{e}^{\mathrm{i}2\pi f t})\,. \tag{8}$$

The calculation of the fourth power, and especially the solution, would be 'distressful'. Nevertheless, we suppose $T_1(0) \ll T_0$ (i.e., the changes of the temperature are small with repsect to the mean temperature) and *linearize* Eq. (8) as $(T_0+T_1)^4 = T_0 + 4T_0^3T_1 + \mathcal{O}(T_1^2)$. We subtract the terms with T_0 and $\mathcal{E}_0$ (they correspond exactly to the equilibrium temperature in Eq. (1)) and we are left with a linear equation for $T_1(0)$:

$$(1+\mathrm{i})\sqrt{\pi f K C\rho}\,T_1(0) + 4\epsilon\sigma T_{\mathrm{eq}}^3\,T_1(0) = (1-A)\mathcal{E}_1\,.$$

The surface temperature is expressed as:

$$T(0,t) = T_{\mathrm{eq}} + \frac{(1-A)\mathcal{E}_1\,\mathrm{e}^{\mathrm{i}2\pi f t}}{(1+\mathrm{i})\sqrt{\pi f K C\rho} + 4\epsilon\sigma T_{\mathrm{eq}}^4}\,.$$

The denominator is a complex number (it means a phase shift); after an algebra we see that:

$$T(0,t) = T_{\mathrm{eq}} + \frac{(1-A)\mathcal{E}_1}{4\epsilon\sigma T_{\mathrm{eq}}^3}\,\frac{1}{1+2\Theta+2\Theta^2}\,\mathrm{e}^{\mathrm{i}(2\pi f t+\phi_{\mathrm{th}})}\,, \tag{9}$$

where the thermal parameter Θ and phase lag ϕ_{th} are:

$$\Theta = \frac{\sqrt{\pi f K C\rho}}{4\pi\epsilon\sigma T_{\mathrm{eq}}^3}\,, \quad \tan\phi_{\mathrm{th}} = -\frac{\Theta}{1+\Theta}\,. \tag{10}$$

For sake of completeness we can write the temperature at a depth (however, it is not crucial for us, because the dynamical action is driven by $T(0,t)$ only):

$$T(x,t) = T_{\mathrm{eq}} + \frac{(1-A)\mathcal{E}_1}{4\epsilon\sigma T_{\mathrm{eq}}^3}\,\frac{1}{1+2\Theta+2\Theta^2}\,\mathrm{e}^{\mathrm{i}(2\pi f t+\phi_{\mathrm{th}}-\sqrt{\pi f/\chi}\,x)}\,\mathrm{e}^{-\sqrt{\pi f/\chi}\,x}\,. \tag{11}$$

There are two visualisations of this steady-state solution (Eq. 11) of the 1-dimensional heat diffusion equation (Eq. 4) in Figures 25 and 26. Thermal properties of materials, from which asteroids probably consist, are listed in Table 5. The summary of the thermal lag ϕ_{th} values (Eq. 10) and the temperature amplitude values $T_1(0)$ (Eq. 9) for typical diurnal and seasonal frequencies is provided in Table 6. The ratio $T_1(0)/T_{\mathrm{eq}}$, which is of the order $\simeq 0.1$ in some cases, tells us, that we are just approaching the limits of the linear theory and the temperature in a full non-linear theory might differ, probably by $\simeq 10\,\%\cdot T_1$.

Knowing the surface temperature T (on an object of any shape), we calculate the elementary radiation force due to the emission of photons, carrying the momentum away from the single surface element $\mathrm{d}S$, as:

$$\mathrm{d}\mathbf{F}_{\mathrm{Y}} = -\frac{2}{3}\frac{\epsilon\sigma T^4}{c}\mathrm{d}S\mathbf{n}_{\perp}\,. \tag{12}$$

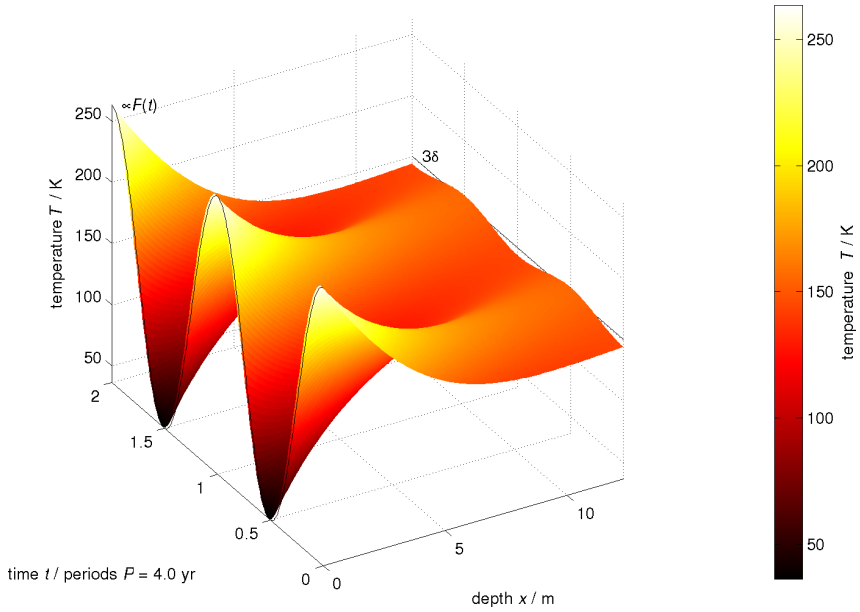

Figure 25: A 3-D plot of the depth x vs. time t vs. temperature T as resulted from the 1-dimensional toy model (Eq. 11). The material properties correspond to a basaltic rock (see Table 5), with the thermal conductivity $K = 1\,\mathrm{W/m/K}$. The flux amplitude $\mathcal{E}_1$ is one half of the equilibrium flux $\mathcal{E}_0$ at 2.5 AU from the Sun; the frequency of the flux $\mathcal{E}(t)$ corresponds to the orbital period of $P = 4\,\mathrm{y}$. The flux is plotted as a thin line in the (t, T) plane and it is scaled the same as the amplitude of the surface temperature $T_1(0)$. The thermal lag between the incident flux $\mathcal{E}(t)$ and the surface temperature $T(0, t)$ is then clearly visible ($\phi_{\mathrm{th}} \doteq -4°$).

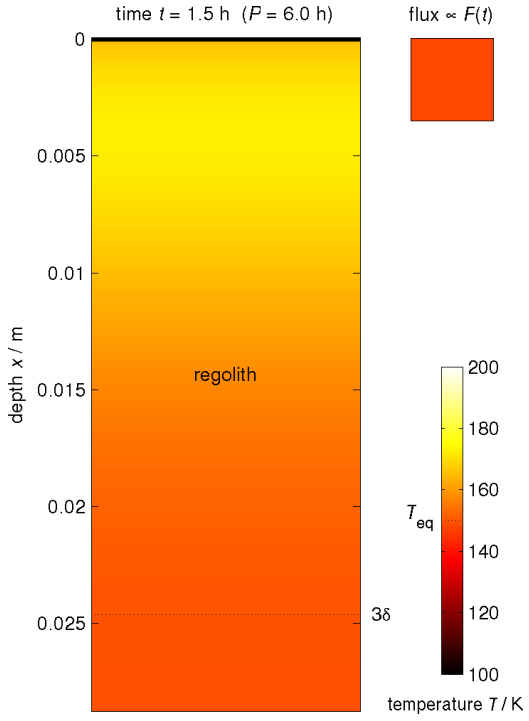

Figure 26: An estimate of the temperature T (colour coded) in the depth x (vertical coordinate) — some sort of "an asteroid cross-section" — for a regolith-like material with the thermal conductivity $K = 0.01\,\mathrm{W/m/K}$ (see Table 5). The situation depicted here corresponds to the 1-D toy model (Eq. 11), with the flux $\mathcal{E}(t)$ period $P = 1/f = 6$ hours, i.e., a typical diurnal motion, and the particular time $t = 1.5\,\mathrm{h}$. The dotted line denotes the depth 3δ, where $\delta = \sqrt{\chi/(\pi f)}$ is the characteristic penetration depth of the thermal wave. There is a colour coded flux $\mathcal{E}(1.5\,\mathrm{h})$, scaled similarly as T, in the upper right square.

Table 6: The penetration depth of the thermal wave δ (Eq. 7), the thermal parameter Θ (Eq. 10), the thermal lag $\phi_{\rm th}$ (Eq. 10) and the amplitude of the surface temperature $T_1(0)$ (Eq. 9) as resulted from the 1-dimensional toy model. The flux amplitude $\mathcal{E}_1$ is one half of the equilibrium flux $\mathcal{E}_0$ at 2.5 AU from the Sun ($T_{\rm eq} \doteq 170\,{\rm K}$). The values were calculated for two types of material (taken from Table 5) and two different periods $P = 1/f$ of the flux $\mathcal{E}(t)$ — a typical diurnal (6 hours) and a seasonal (4 years).

material	P	δ	Θ	$\phi_{\rm th}$	$T_1(0)$
		m		deg	K
basalt	6 h	0.05	6	−40	1
	4 y	4	0.08	−4	82
regolith	6 h	0.008	0.4	−15	47
	4 y	0.6	0.005	−0.3	94

The factor $\frac{2}{3}$ conforms to the Lambert law of scatterring; $\mathbf{n}_\perp$ denotes the external normal unit vector. The Yarkovsky acceleration of a homogeneous body with the total mass m is then given by the integration over the whole surface:

$$\mathbf{a}_{\rm Y} = -\frac{2}{3}\frac{\epsilon\sigma}{mc}\int_S {\rm d}S\,\mathbf{n}_\perp T^4 \simeq -\frac{8}{3}\frac{\epsilon\sigma}{mc}T_{\rm eq}^3\int_S {\rm d}S\,\mathbf{n}_\perp T_1\,, \tag{13}$$

where we can use the linearization of T^4 again.

Similarly, we express the total YORP torque (affecting the spin of the body):

$$\mathbf{T}_{\rm Y} = \int_S \mathbf{r}\times{\rm d}\mathbf{F}_{\rm Y} = -\frac{2}{3}\frac{\epsilon\sigma}{c}\int_S \mathbf{r}\times\mathbf{n}_\perp {\rm d}S\,T^4\,. \tag{14}$$

The major orbital perturbation caused by $\mathbf{a}_{\rm Y}$ is the semimajor axis drift. The first Gauss equation reads:

$$\frac{{\rm d}a}{{\rm d}t} = \frac{2\mathcal{T}}{n} + \mathcal{O}(e)\,, \tag{15}$$

where $\mathcal{T}$ denotes the transversal component of $a_{\rm Y}$. As we can see from Eq. (13), the resulting total transverse acceleration $\mathcal{T}$ (hence, the semimajor axis drift rate ${\rm d}a/{\rm d}t$) is: i) proportional to the *deviations* of temperature from the equilibrium, ii) the sine of the thermal lag angle $\sin\phi_{\rm th}$ (see Figure 27), and iii) inversely proportional to the size (because $F_{\rm Y} \propto$ surface area S and $a_{\rm Y} = \frac{F}{m}$).[1]

The YORP torque $\mathbf{T}_{\rm Y}$ changes the angular momentum L of the body: $\frac{{\rm d}\mathbf{L}}{{\rm d}t} = \mathbf{T}_{\rm Y}$. In case the body rotates around the shortest axis of the inertia tensor, then $\mathbf{L} = C\omega\mathbf{e}$, where C denotes the moment of inertia (assumed constant), ω the angular velocity and $\mathbf{e}$ the unit vector along the spin axis. The rate of change of $\mathbf{L}$ is usually expressed in three angular variables:

$$\frac{{\rm d}\omega}{{\rm d}t} = \frac{\mathbf{T}\cdot\mathbf{e}}{C}\,, \tag{16}$$

$$\frac{{\rm d}\gamma}{{\rm d}t} = \frac{\mathbf{T}\cdot\mathbf{e}_{\perp 1}}{C\omega}\,, \qquad \mathbf{e}_{\perp 1} = \frac{(\mathbf{N}\cdot\mathbf{e})\,\mathbf{e} - \mathbf{N}}{\sin\gamma}\,, \tag{17}$$

$$\frac{{\rm d}\psi}{{\rm d}t} = \frac{\mathbf{T}\cdot\mathbf{e}_{\perp 2}}{C\omega}\,, \qquad \mathbf{e}_{\perp 2} = \frac{\mathbf{e}\times\mathbf{N}}{\sin\gamma}\,, \tag{18}$$

where γ is the obliquity, ψ the longitude, $\mathbf{T}$ the total torque (aside the YORP one, there are usually gravitational torques and inertial terms due to the motion of the reference frame), the unitvector $\mathbf{N}$ is perpendicular to the orbital plane. $\frac{{\rm d}\omega}{{\rm d}t}$ scales as $\frac{1}{R^2}$ (because $T_{\rm Y} \propto R^3$ and $C \propto R^5$).[2]

[1] A typical magnitude of the radiation force per $1\,{\rm m}^2$ could be ${\rm d}F_{\rm Y} \doteq \frac{2}{3}\frac{0.9\cdot 5.67\cdot 10^{-8}\cdot 160^4\cdot 1}{3\cdot 10^8}\,{\rm N} \doteq 10^{-7}\,{\rm N}$. For a typical 1-km asteroid, we have roughly (see the parameters for the regolith material and the diurnal frequency in Table 6): $a_{\rm Y} \doteq \frac{8}{3}\frac{0.9\cdot 5.67\cdot 10^{-8}\cdot 160^3}{(4/3)\cdot 3.14\cdot 1000^3\cdot 3500\cdot 3\cdot 10^8}\,4\cdot 3.14\cdot 1000^2\cdot 47\,{\rm m\cdot s^{-2}} \doteq 10^{-13}\,{\rm m\cdot s^{-2}}$ (compare it to the gravitational acceleration $a_{\rm G} = \frac{GM_\odot}{r^2} \doteq 10^{-3}\,{\rm m\cdot s^{-2}}$); the transverse component $\mathcal{T} \doteq 10^{-13}\cdot\sin 15^\circ\,{\rm m\cdot s^{-2}} \doteq 10^{-14}\,{\rm m\cdot s^{-2}}$, the mean motion $n = \sqrt{\frac{GM_\odot}{a^3}} \doteq 0.004\,\frac{\rm rad}{\rm day}$ and the resulting semimajor axis drift rate $\frac{{\rm d}a}{{\rm d}t} \doteq \frac{2\cdot 10^{-14}\cdot(86400^2/150\cdot 10^9)}{0.004}\cdot 365.25\cdot 10^6\,\frac{\rm AU}{\rm My} \doteq 10^{-4}\,\frac{\rm AU}{\rm My}$. These order-of-magnitude estimates are consistent with a more complex 3-D modelling (see Section 2.3.2, Figure 29).

[2] A crude estimate of the YORP torque acting on a 1-km asteroid with an irregular shape might be $T_{\rm Y} = |\int_S \mathbf{r}\times{\rm d}\mathbf{F}_{\rm Y}| \doteq 1000\cdot 10^{-7}\cdot 10^{-2}\cdot 4\cdot 3.14\cdot 1000^2\,{\rm N\cdot m} \doteq 10^1\,{\rm N\cdot m}$. (Here, we naively assumed that 1 % of the whole surface area radiates in

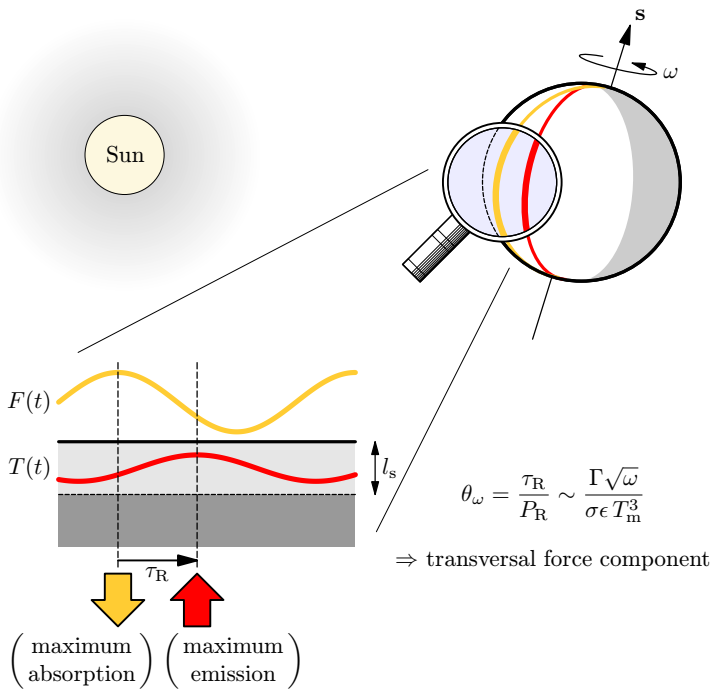

Figure 27: The time lag between the absorption of the solar radiation and the thermal emission arising on a rotating spherical body. The incident solar flux $F(t)$ is maximum at the subsolar point, but the maximum emission takes place somewhat later due to the rotation. Therefore, the radiation force has a non-zero tranversal component, which is proportional to the sine of the thermal lag angle $\sin\phi_{\rm th}$ (measured between the yellow and red semicircles on the sphere).

There are two important aspects we could not account for in the 1-D model above: i) the finite size of the body, and ii) the dependence on the obliquity. If the size is of the order δ or smaller, the conduction of heat across the body effectively equilibrates the surface temperature and thus spherically symmetric bodies are not accelerated any more.

The obliquity γ (i.e., the angle between the rotational axis and the normal to the orbital plane) is also an important parameter. Let us imagine a sphere orbiting the Sun (Figure 28) and distinguish three special cases:

1. The prograde diurnal rotation ($\gamma = 0°$) and the inevitable thermal lag give rise to a non-zero transverse component $\mathcal{T}_{\rm Y}$ of the Yarkovsky acceleration, which causes the body to spiral away from the Sun (semimajor axis steadily increases, in agreenment with the Gauss equation $\frac{{\rm d}a}{{\rm d}t} \doteq \frac{2\mathcal{T}}{n}$).
2. On the contrary, the retrograde rotation ($\gamma = 180°$) forces the semimajor axis to decrease.
3. The spin axis tilted in the orbital plane ($\gamma = 90°$) means, there are large seasonal temperature variations and the corresponding thermal lag (calculated for the orbital frequency) leads to a steady decrease of semimajor axis (regardless on the sense of the diurnal rotation).

Both the dependence on size and obliquity arise naturally in 3-dimensional models (see Section 2.3.2).

2.3.2 A spherically symmetric linear model.

An analytical solution of the heat diffusion equation with a linearized boundary condition is also possible for a sphere and an appropriate solar flux $\mathcal{E}(t)$ (Vokrouhlický (1998), Vokrouhlický & Farinella (1999), Vokrouhlický (1999)). Hereinafter, we use scaled quantities (denoted by dashes): $r' = r/l_{\rm s}$,

one direction tangent to the surface.) The moment of inertia is approximately $C = \frac{8}{15}\pi R^5\rho \doteq 5\cdot 10^{18}\,{\rm kg}\cdot{\rm m}^2$. Therefore, $\frac{{\rm d}\omega}{{\rm d}t} \doteq \frac{10^1}{5\cdot 10^{18}}\,\frac{\rm rad}{\rm s^2} = 2\cdot 10^{-18}\,\frac{\rm rad}{\rm s^2}$. What is the timescale for a complete spin-down? If we start with $\omega_0 = 3\cdot 10^{-4}\,\frac{\rm rad}{\rm s} \doteq 5\,\frac{\rm rev}{\rm day}$, then $\tau_\omega \doteq \frac{3\cdot 10^{-4}}{2\cdot 10^{-18}}\,{\rm s} = 1.5\cdot 10^{14}\,{\rm s} \doteq 10^7\,{\rm y}$. (The timescale for a spin-up is of the same order, because the upper limit is $\omega_{\rm crit} \doteq 11\,\frac{\rm rev}{\rm day}$; if the rotation is faster, gravitationally bound bodies likely disintegrate.) Similarly, $\frac{{\rm d}\gamma}{{\rm d}t} \doteq \frac{10^1}{5\cdot 10^{18}\cdot 3\cdot 10^{-4}}\,\frac{\rm rad}{\rm s} \doteq 10^{-14}\,\frac{\rm rad}{\rm s}$ and a $\frac{\pi}{2}$ change of the tilt can be expected after $\tau_\gamma \doteq \frac{1.57}{10^{-14}}\,{\rm s} \doteq 10^7\,{\rm y}$.

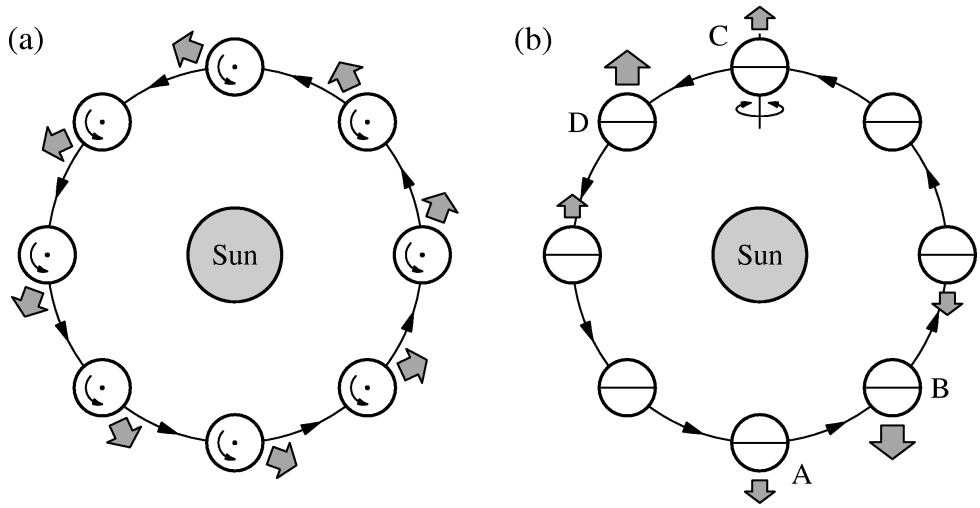

Figure 28: Diurnal and seasonal variants of the Yarkovsky effect and the dependence on the obliquity γ. The gray arrows denote the recoil force acting on the body. (a) The diurnal Yarkovsky effect, when the body rotates around the spin axis perpendicular to the orbital plane. In this case of prograde rotation, the force causes an increase of the semimajor axis a. Generally, the change $\Delta a \propto \cos\gamma$. (b) The seasonal Yarkovsky effect, with the spin axis in the orbital plane. The heating of the hemispheres, mainly at points A and C, and the delayed emission of thermal radiation, mainly at points B and D, produce a recoil force, which magnitude changes along the orbit, but which transverse component is always opposite to the velocity, thus causing a steady decrease of the semimajor axis ($\Delta a \propto -\sin^2\gamma$).

$l_\mathrm{s} = \sqrt{K/\rho C\omega_\mathrm{rev}}$, $\Delta T' = \Delta T/T_\star$, $\epsilon\sigma T_\star^4 = \alpha\mathcal{E}_\star$, $\alpha = (1-A)$, $\Delta\mathcal{E}' = \Delta\mathcal{E}/\mathcal{E}_\star$, $\Delta\mathcal{E} = \mathcal{E} - \mathcal{E}_\star/4$, $\zeta = \mathrm{e}^{\mathrm{i}\lambda}$, $\lambda = \omega_\mathrm{rev}(t-t_0)$. The flux can be written easily in terms of spherical harmonics:

$$\Delta\mathcal{E}' = \sum_{n\geq 1}\sum_{k=-n}^{n} a_{nk}(\zeta)\, Y_{nk}(\theta,\phi)\,. \tag{19}$$

We need three dipole terms only (to express the flux differs from zero on the illuminated hemisphere only):

$$a_{10}(\zeta) = \sqrt{\frac{\pi}{3}}\,\cos\theta_0\,, \qquad a_{1\pm1}(\zeta) = \mp\sqrt{\frac{\pi}{6}}\,\sin\theta_0\, e^{\mp i\phi_0}\,, \tag{20}$$

where (θ_0,ϕ_0) are the coordinates of the Sun, which in turn change periodically with time, according to $\cos\theta_0 = -\sin\gamma\sin\lambda = \frac{i}{2}\sin\gamma(\zeta-\zeta^{-1})$, $\sin\theta_0\, e^{\pm i\phi_0} = -(\sin^2\frac{\gamma}{2}\,\zeta^{\mp(m+1)} + \cos^2\frac{\gamma}{2}\,\zeta^{\mp(m-1)})$, where γ is the obliquity.

The heat diffusion equation and the boundary condition (Eqs. 2 and 3) in spherical coordinates (and after the linearization) now read:

$$i\zeta\frac{\partial}{\partial\zeta}\Delta T'(r';\theta,\phi;\zeta) = \frac{1}{r'^2}\left\{\frac{\partial}{\partial r'}\left(r'^2\frac{\partial}{\partial r'}\right) + \frac{1}{\sin\theta}\left[\frac{\partial}{\partial\theta}\left(\sin\theta\frac{\partial}{\partial\theta}\right) + \frac{1}{\sin\theta}\frac{\partial^2}{\partial\phi^2}\right]\right\}\Delta T'(r';\theta,\phi;\zeta)\,, \tag{21}$$

$$\sqrt{2}\Delta T' + \Theta\left(\frac{\partial\Delta T'}{\partial r'}\right)_{R'} = \Delta\mathcal{E}'\,. \tag{22}$$

It is convenient to look for a solution T', which has a the same structure as the source flux (Eq. 19):

$$\Delta T'(r';\theta,\phi;\zeta) = \sum_{n\geq 1}\sum_{k=-n}^{n} t'_{nk}(r';\zeta)\, Y_{nk}(\theta,\phi)\,. \tag{23}$$

The properties of the Eqs. (21) and (22) (namely the orthogonality of the Y_{nk} functions) lead to a complete separation of radial, angular and time variables and even individual Fourier modes. Vokrouhlický (1999) found the solution for the three necessary dipole coefficients $t'_{10}(R';\zeta)$ and $t'_{1\pm1}(R';\zeta)$. (We do not write them explicitly here, but see Sec. 2.3.3.)

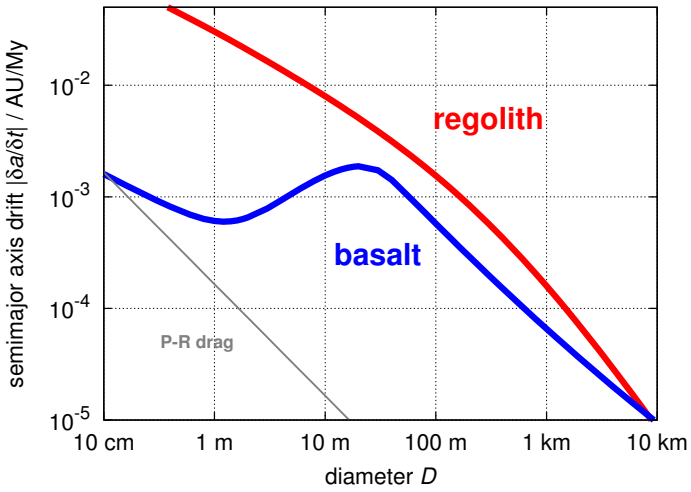

Figure 29: The sum of absolute values $|\mathrm{d}a/\mathrm{d}t|$ of the diurnal and the seasonal semimajor axis drift rates vs. size, calculated for spherical bodies with a moderate value of obliquity $\gamma = 135^\circ$ and consisting of two materials from Table 5: bare basalt and regolith covered, i.e., with high and low thermal conductivity. (Of course, for particular values of γ the diurnal or the seasonal Yarkovsky effect may vanish; they can even cancel each other, when the diurnal rate is positive and the seasonal negative.) Nevertheless, the sum plotted here shows clearly an approximate maximum total drift (per 1 My) one can expect. The mean collisional lifetime is roughly 50 My for a 10-m stony meteoroid and 500 My for a 1-km asteroid (Farinella *et al.* (1998), Bottke *et al.* (2005b)). Note, that we do not expect very small regolith-covered bodies to exist, thus the drift rates larger than 10^{-2} AU/My are not realistic. The drift rate caused by the Poynting-Robertson drag is also plotted; it prevails for sizes smaller than $\lesssim 10$ cm.

The Yarkovsky acceleration is given by the integration over the surface of the sphere:

$$\mathbf{f}(\zeta) = -\frac{2\sqrt{2}}{3\pi}\alpha\,\Phi \int \mathrm{d}\Omega\,\Delta T'(R';\theta,\phi;\zeta)\,\mathbf{n}\,, \tag{24}$$

where $\Phi = (\mathcal{E}_\star \pi R^2/mc)$. We obtain the following expressions for the components (f_X, f_Y, f_Z):

$$f_X(\zeta) + \mathrm{i} f_Y(\zeta) \;=\; -\frac{8}{3\sqrt{3\pi}}\,\alpha\,\Phi\,t'_{1-1}(R';\zeta)\,, \tag{25}$$

$$f_Z(\zeta) \;=\; -\frac{4}{3}\sqrt{\frac{2}{3\pi}}\,\alpha\,\Phi\,t'_{10}(R';\zeta)\,. \tag{26}$$

The equatoreal components (in the XY plane) are called diurnal (because it depends mainly on the rotational frequency), while the along-axis component is called seasonal (because of the orbital frequency). Note, there is zero YORP torque (Eq. 14) within spherical models.

In order to find secular effects of the Yarkovsky acceleration on the semimajor axis, we have to transform it to the heliocentric reference frame, substitute to the Gauss equation $\mathrm{d}a/\mathrm{d}t = 2\mathcal{T}/\omega_{\mathrm{rev}}$ and average over one orbit. The results for the diurnal and seasonal components are of the form:

$$\left(\frac{\mathrm{d}a}{\mathrm{d}t}\right)_{\mathrm{d}} \;\simeq\; -\frac{8\alpha}{9}\,\frac{\Phi}{\omega_{\mathrm{rev}}}\,\frac{E_{R'_m}\sin\delta_{R'_m}}{1+\chi}\,\cos\gamma\,, \tag{27}$$

$$\left(\frac{\mathrm{d}a}{\mathrm{d}t}\right)_{\mathrm{s}} \;=\; \frac{4\alpha}{9}\,\frac{\Phi}{\omega_{\mathrm{rev}}}\,\frac{E_{R'}\sin\delta_{R'}}{1+\chi}\,\sin^2\gamma\,. \tag{28}$$

The dependence of $\mathrm{d}a/\mathrm{d}t$ on the obliquity (discussed already within the 1-D toy model in Section 2.3.1) is recalled here. An example, how the semimajor axis drift rates depend on size is depicted in Figure 29.

2.3.3 The implementation in the `swift_rmvsy` package

Most of the simulations of the long-term orbital evolution presented in Sections 2.3.4 to 7 exploit the spherical linear model of the Yarkovsky acceleration (Sec. 2.3.2). In our previous work (Brož, 1999) we modified